

Electromagnetic shielding efficiency of hybrid knitted fabrics treated with mxene

Volume 54: 1–21
© The Author(s) 2024
Article reuse guidelines:
sagepub.com/journals-permissions
DOI: 10.1177/15280837241279963
journals.sagepub.com/home/jit



Hamed Mohammadi Mofarah , Mutalifu Abulikemu,
Bitá E. A. Tabrizi, Hyung Woo Choi and Ghassan E. Jabbour

Abstract

This study details the fabrication of a hybrid fabric structure achieved through the utilization of copper-cotton core-spun yarns and a streamlined dip-coating method for the coating of MXene sheets. This fabrication approach results in a substantial enhancement in electromagnetic interference shielding efficiency (EMI SE) in the X-band frequency (8.2–12.4 GHz) while significantly reducing the required number of MXene coating steps. The textile samples fabricated with 0.08 mm diameter copper core filaments and a knitting density of 12 gauge (needle/inch) exhibit a peak EMI SE of 43.9 dB following three MXene coating cycles, utilizing a 1×1 Rib knit pattern. In comparison, employing a Full Milano knit pattern results in an improved EMI SE, reaching up to 45.2 dB. These findings elucidate the substantial impact of knit structure and the effective MXene coating process on improving the EMI SE for hybrid textiles.

Keywords

MXene, electromagnetic interference (EMI) shielding efficiency (SE), copper cotton, dip-coating, knitted fabric

School of Electrical Engineering and Computer Science, University of Ottawa, Ottawa, ON, Canada

Corresponding author:

Ghassan E. Jabbour, School of Electrical Engineering and Computer Science, University of Ottawa, 800 King Edward Ave, Ottawa, ON K1N 6N5, Canada.

Email: gja@uottawa.ca



Creative Commons Non Commercial CC BY-NC: This article is distributed under the terms of the Creative Commons Attribution-NonCommercial 4.0 License (<https://creativecommons.org/licenses/by-nc/4.0/>) which permits non-commercial use, reproduction and distribution of the work without further permission provided the original work is attributed as specified on the SAGE and Open Access pages (<https://us.sagepub.com/en-us/nam/open-access-at-sage>).

Introduction

The unique properties of textiles, such as their fibrous and porous structure, coupled with their inherent breathability, flexibility, and comfort, have sparked increasing interest in the field of wearable and smart electronics. The rapid growth of this subject has motivated researchers to create new and improved technologies in the area of intelligent textile-based electronics, utilizing the unique properties of textiles to construct sophisticated and user-friendly solutions.^{1–3} Smart wearables and textiles have been created for a range of purposes, like electromagnetic interference shielding,^{4,5} energy harvesting and storage,⁶ thermal management,⁴ sensors,⁷ and wearable robots.⁸ Different materials have been used to prepare technical, multifunctional, and smart fabrics, including metal nanomaterials,⁹ carbon nanotubes,¹⁰ carbon black,¹¹ graphene,¹² and conductive polymers.^{13–15} Various methods are used to functionalize the textiles with the above-mentioned materials. Among those methods, spray coating,¹⁶ dip coating,⁴ and screen printing¹¹ have gained more attention.

The rapid growth of wireless communication and electronic devices has raised concerns over the environmental consequences of electromagnetic wave pollution. The development of highly efficient EMI shielding materials has become necessary in order to mitigate the adverse impacts of EMI. Electrically conductive textiles, due to their natural fibrous and porous characteristics, as well as their breathability and flexibility, are gaining interest in many EMI shielding applications. Nevertheless, there is typically a negative correlation between the thickness of the conductive coating and the flexibility of the fabric. As the thickness increases, the fabric's elasticity and breathability tend to diminish, which undermines its comfort and wearability. In contrast, increasing the thickness of the conductive layer generally improves the EMI SE, providing superior defense against electromagnetic pollution. This presents a notable difficulty: attaining an ideal balance between the mechanical flexibility and the electromagnetic interference shielding efficiency of fabrics coated with conductive material. Therefore, the current and crucial topic of study involves improving the design of conductive materials that preserve fabric flexibility while reaching acceptable levels of EMI SE.

Because of their lightweight and excellent electrical conductivity, two-dimensional (2D) transition-metal carbides and nitrides (MXenes) have attracted the interest of EMI SE researchers.¹⁷ MXene's chemical formula is $M_{n+1}X_nT_x$; M represents an early transition metal such as Ti, V, Mo, Cr, and Zr, X stands for carbon and/or nitrogen, and T_x stands for functional groups (O, F, OH), and $n = 1, 2, 3$. MXene is often synthesized by selectively etching from MAX phase powder,¹⁸ where A is often aluminum (Al), silicon (Si), or gallium (Ga). Due to its improved mechanical qualities, high electrical conductivity (10000 S/cm), and polar surfaces, $Ti_3C_2T_x$ was found to have an advantage over other forms of MXenes.^{19–23}

Yin et al. employed a layer-by-layer technique to deposit polyaniline nanowires and MXene onto a carbon fiber fabric, achieving an EMI SE of 35.3 dB after a series of 50 coating cycles with an MXene concentration fine-tuned to 5 mg mL⁻¹.²⁴ Remarkably, the EMI SE reached the threshold of 60 dB when utilizing three samples of the coated fabric layered together. In a similar vein, Li et al. fabricated a polyaniline/MXene/cotton

textile, maintaining the MXene concentration at 5 mg mL^{-1} while varying the polyaniline concentrations across 1, 2, and 3 mg mL^{-1} . It was observed that increasing the polyaniline concentration in conjunction with the number of coating cycles, from 5 to 30, proportionally enhanced the EMI shielding capabilities of the textile. In this case, an EMI SE of 54 dB was reported.²⁵ Dong et al. utilized an airbrush to cover the thermoplastic polyurethane (TPU) fabric with a 2 mg mL^{-1} aqueous solution of MXene. The coating process was methodically carried out to incrementally enhance the MXene loading on the fabric samples to 3, 6, 9, and 12 mg. As a result, increasing the MXene content from 3 mg to 12 mg led to a substantial rise in the EMI SE, which soared from 14.2 dB to an impressive 31.4 dB.²⁶ Lan et al. increased the EMI SE of cotton fabric via 10-cycle dip-coating process of MXene and polyethyleneimine (PEI) (10 cycles). MXene concentrations of 5, 10, and 20 mg mL^{-1} were used, as well as three different PEI concentrations (0.5, 1, and 3 mg mL^{-1}). Samples containing 1 mg mL^{-1} PEI and MXene performed best. In this case, increasing the coating cycles from 5 to 20 for samples containing 10 mg mL^{-1} MXene and 1 mg mL^{-1} PEI enhanced the EMI SE from 10 to 27.32 dB. Furthermore, for the 1 mg mL^{-1} PEI and 10-cycle coating, raising the concentration of MXene from 5 mg mL^{-1} to 20 mg mL^{-1} raised the EMI SE from 7 to 25.28 dB.²⁷ Using spray coating of a 2 mg mL^{-1} aqueous MXene solution on cotton fabric, Zhang et al. demonstrated the EMI SE of 25, 33, and 36 dB for textile samples having 12, 23, and 35 coating cycles, respectively.²⁷

To achieve a textile with significant EMI SE, it is usually necessary to apply several coatings. However, this procedure can be resource-intensive, requiring a significant amount of time, energy, and materials. In order to address this lack of efficiency, it is crucial to build a novel framework that can achieve similar levels of EMI SE with a reduced number of coating applications. Such a structure would represent a significant advancement by optimizing resource utilization while delivering high-performance shielding. In this context, our approach relied on using hybrid knitted textiles based on copper-cotton core-spun yarn, and 2D MXene nanosheets deposited onto the hybrid fabric using a dip-coating technique. Copper is more ductile and flexible than stainless steel filaments. Consequently, copper filaments can bend more easily under the same amount of force compared to stainless steel filaments, making copper a better candidate for fabricating hybrid knitted fabric. Furthermore, copper and MXene are both highly conductive and desirable in EMI SE applications^{28,29}; combining them in the textile structure will synergistically improve total EMI SE. To assess the impact of copper filament on EMI SE, we tested a plain knitted cotton fabric that contained no copper filament or MXene coating. As shown in [Figure S1](#), the EMI SE of this plain knitted cotton fabric in the 8.2-12.4 GHz frequency range was negligible, effectively measuring at 0.

In this investigation, the X-band frequency range was selected for the in-depth analysis of the EMI SE of the samples under study. This frequency range is characterized by a shallow penetration depth in various materials, ensuring that the interaction of electromagnetic waves occurs predominantly at the material surface. This characteristic is advantageous for precise evaluation of the efficacy of surface-level shielding. Moreover, the prevalence of X-band frequencies in the operational spectrum of radar and communication devices makes them particularly suitable for assessing the EMI SE in applications relevant to real-world scenarios.

In this study, the hybrid knitted fabrics using copper filaments and cotton fibers, coated with MXene to enhance EMI SE were developed. The unique aspect of our work lies in combining copper and MXene, both known for their high conductivity. This combination creates a synergistic effect, significantly boosting the fabric's conductivity and, consequently, its EMI SE. Previous studies have primarily used stainless steel filaments in knitted fabrics, achieving EMI SE values around 20 dB within the frequency range of 0.3 to 1.5 GHz.^{30,31} Three-layer laminations of knitted fabrics containing HS-PET filaments, stainless steel (SS) wires, and bamboo charcoal fibers achieved the EMI SE of less than 30 dB in the frequency range from 0-3 GHz.³² In contrast, our research targets the X-band frequency range (8.2-12.4 GHz), a considerably higher frequency range. Our results demonstrate a much higher EMI SE than these earlier works. By incorporating copper and MXene into our fabric design, we have achieved superior EMI SE performance across a broader and higher frequency spectrum, marking a significant advancement in this field.

The primary aim of this research is to reduce the number of MXene coating cycles while maintaining or potentially improving EMI SE. Additionally, the study aims to investigate the impact of fabric density on EMI SE by using three distinct machine gauges that provide varying fabric densities. This research used Full Milano and 1×1 Rib knit patterns to examine the effect of knit patterns on EMI SE. The Full Milano fabric offers a greater thickness and density compared to the 1×1 Rib knit design. Additionally, this study employed three distinct copper filament sizes to examine the effect of increasing copper filament diameter on EMI SE. The research resulted in the creation of a fabric that demonstrated an outstanding EMI SE of 45.2 dB. This achievement was accomplished after only three cycles of dip-coating, highlighting the efficiency of the refined coating technique.

Experimental section

Materials

The linear density of combed cotton roving was 716 tex. Two rovings were used to prepare the core-sheath yarns. The copper filaments of 0.06, 0.07, and 0.08 mm in diameter were used as the core material in the yarn production process. The mechanical properties of copper filaments are reported in Table 1. MXene powder ($Ti_3C_2T_x$ MXene Few layer Nanoflake with a purity of 99 wt %, and number of layers 1–10) was purchased from Nanochemazone Canada.

Table 1. Mechanical properties of copper filaments.

Diameter (mm)	Tensile stress (MPa)	Tensile strain (%)
0.06	1541.65 ± 0.52	2.53 ± 1.65
0.07	1900.74 ± 0.76	2.22 ± 1.42
0.08	2567.27 ± 1.02	1.99 ± 1.29

Preparation of copper-cotton core-spun yarns and knitted fabrics

In the production of core-spun yarns utilizing copper filaments with varying diameters (0.06, 0.07, and 0.08 mm), the Siro spinning method was chosen. To execute this process, a conventional spinning machine underwent modifications to accommodate the specific requirements of yarn production. The introduction of a disk tensioner and a porcelain guide facilitated the controlled feeding of copper filament from the package to the nip line of the front roller. To further refine the process, a roving condenser was employed to separately direct the rovings to the draft zone of the spinning machine. Additionally, a condenser positioned behind the front roller was incorporated to consolidate the two rovings into a singular structure. Ensuring precise positioning of the copper filament within the yarn necessitated the implementation of pretension. This critical aspect was addressed by setting pretension values at 20, 30, and 33 g for copper filaments with diameters of 0.06 mm, 0.07 mm, and 0.08 mm, respectively. Figure 1(a) provides a schematic representation of the Siro spinning method, illustrating the key components and the sequential flow of the manufacturing process.³³

Production of Knitted fabrics

This investigation utilized a flat double bed knitting machine with three distinct gauges (8, 10, and 12 needle per inch) to generate two knit patterns, namely 1×1 Rib and Full Milano. Figure 1 provides a visual representation of the loop notation for the knit structures, accompanied by light microscopy images depicting the characteristics of 1×1 Rib and Full Milano knit patterns.³⁴ A total of eighteen fabric samples were systematically manufactured, encompassing the combination of 2 knit patterns, 3 machine gauges, and 3 different yarns derived from copper filaments (refer to T1–T18 in Table 2).

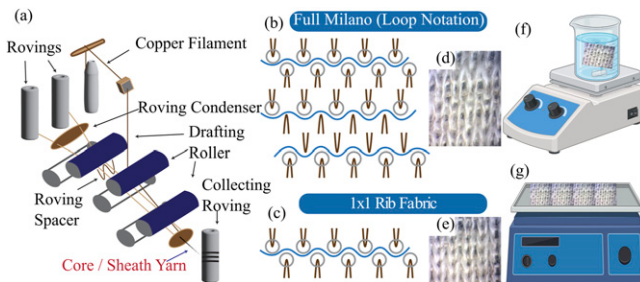


Figure 1. Schematic illustration of fabricated textiles, a) Schematic illustration of copper-cotton core-spun yarn using the Siro method. (b) loop notations of Full Milano, (c) loop notations of 1×1 Rib, (d) photo of Full Milano fabric, (e) photo of 1×1 Rib fabric, (f) Schematic illustration of the dip coating process of fabric in the aqueous solution of MXene, and (g) Schematic illustration of drying fabric on the hot plate.

Table 2. Fabric specifications and allocated sample codes.

Gauge	Copper Diameter (mm)	Untreated	Fabric Thickness (mm)	1-Cycle Coating	2-Cycle Coating	3-Cycle Coating
8	0.06	T1: Full Milano	1.32	T19: Full Milano		
		T2: 1 x 1 Rib	0.87	T20: 1 x 1 Rib		
	0.07	T3: Full Milano	1.45	T21: Full Milano		
		T4: 1 x 1 Rib	1.29	T22: 1 x 1 Rib		
	0.08	T5: Full Milano	1.51	T23: Full Milano	T37: Full Milano	T43: Full Milano
		T6: 1 x 1 Rib	1.33	T24: 1 x 1 Rib	T38: 1 x 1 Rib	T44: 1 x 1 Rib
10	0.06	T7: Full Milano	1.41	T25: Full Milano		
		T8: 1 x 1 Rib	1.02	T26: 1 x 1 Rib		
	0.07	T9: Full Milano	1.5	T27: Full Milano		
		T10: 1 x 1 Rib	1.31	T28: 1 x 1 Rib		
	0.08	T11: Full Milano	1.55	T29: Full Milano	T39: Full Milano	T45: Full Milano
		T12: 1 x 1 Rib	1.35	T30: 1 x 1 Rib	T40: 1 x 1 Rib	T46: 1 x 1 Rib
12	0.06	T13: Full Milano	1.44	T31: Full Milano		
		T14: 1 x 1 Rib	1.17	T32: 1 x 1 Rib		
	0.07	T15: Full Milano	1.65	T33: Full Milano		
		T16: 1 x 1 Rib	1.34	T34: 1 x 1 Rib		
	0.08	T17: Full Milano	1.68	T35: Full Milano	T41: Full Milano	T47: Full Milano
		T18: 1 x 1 Rib	1.38	T36: 1 x 1 Rib	T42: 1 x 1 Rib	T48: 1 x 1 Rib

Preparation of aqueous MXene solution and samples for coating

Aqueous MXene solutions with a concentration of 10 mg mL^{-1} were formulated. The resulting solution underwent a 2-hour sonication process to effectively delaminate MXene flakes into few-layer MXene sheets. Sonication was conducted in a water bath with a constant temperature maintained at room temperature. Subsequently, fabric samples underwent treatment with isopropyl alcohol (IPA) for 20 min under sonication. Following the treatment process, the samples were thoroughly rinsed using distilled water and subsequently allowed to dry in ambient environment at room temperature. This process aimed to eliminate any residual contaminants originating from the spinning and knitting procedures. [Table 2](#) provides a comprehensive overview of sample specifications, accompanied by assigned codes for each sample. Notably, the Full Milano knit pattern was employed for samples with odd-numbered codes, while the 1×1 Rib knit pattern was used for samples with even-numbered codes.

Polar groups (-O, -OH, and -F) on the surface of MXene sheets provide two functions. First, they improve MXene sheets' hydrophilicity and dispersibility in polar solvents such as DI water. Second, they improve the binding forces between MXene sheets and the cotton surface of prepared textiles, such as the van der Waals force, hydrogen bonding, and electrostatic interaction.³⁵ Dip-coating was used to deposit MXene sheets on hybrid knitted fabrics. Each fabric sample was submerged in a 10 mg mL^{-1} aqueous MXene solution for 2 minutes at room temperature under magnetic stirring at 400 rpm. Magnetic stirring also assisted in preventing the sedimentation of MXene at the bottom of the beaker ([Figure 1\(f\)](#)). The samples were then removed from the solution and fully dried on a hot plate at $70 \text{ }^\circ\text{C}$ ([Figure 1\(g\)](#)) and kept in an ambient atmosphere. As shown in [Table 2](#), the thickest Full Milano and 1×1 Rib samples, which are linked to the samples made with the 0.08 mm copper filament, are chosen to be treated for the second and third cycles of coating in each gauge category (8, 10, and 12 needles per inch). The second and third cycles of the coating were repeated in the same way as the first. [Figure 3](#) illustrates the FESEM picture of the untreated fabric, fabric with 1 cycle, 2 cycles (T37-T42), and 3 cycles (T43-T48) of MXene treatment at various magnifications. A cross-sectional FESEM analysis of sample T47 was conducted to elucidate the penetration depth of the MXene coating within the textile structure, as depicted in [Figure S2](#).

Characterizations

The fabric characterization such as yarn count, fabric thickness, breaking force, and elongation of fabrics were measured in both the lengthwise and widthwise directions and are shown in [Table S1](#). The breaking force and elongation of fabrics were assessed using the ASTM D5034 standard. The specimens were cut into a typical test sample of 50 mm in width and 200 mm in length. The test speed was set to 100 mm min^{-1} . A total of 5 samples were tested and the average was reported as the breaking force, and elongation. [Figure S3](#) shows the schematic of the force application direction, both lengthwise and widthwise, to the fabrics. The thickness of fabrics were measured using Shirley thickness gauge at the pressure of 20 gf cm^2 . The average of 10 different spots on the fabric was reported as the

overall thickness of fabric. The fabrics gram per square meter was measured for each fabric 5 samples of 10 cm × 10 cm was cut and measured. The average was reported as the gram per square meter of fabrics. [Table S1](#) depicts the gram per square meter of fabrics.

Field Emission Scanning Electron Microscope (FESEM, Zeiss Gemini 500) was used to investigate the morphology, microstructure, and distribution of MXene sheets on the hybrid knitted copper-cotton fabrics after one, two, and three layers of MXene coating, followed by elemental analysis using Energy Dispersive Spectroscopy (EDS) in order to determine the chemical components. In addition, the position of copper filaments in the fabric was observed through the cross-section of dip-coated fabric. The elemental bonding properties of the MXene at the interfaces were analyzed using Attenuated Total Reflection Fourier Transform Infrared (ATR-FTIR) Spectroscopy (Thermo Scientific, Nicolet 6700). X-ray diffraction (XRD) analysis was performed on MXene powder, uncoated hybrid fabric, and MXene-coated hybrid fabric to distinguish their crystalline lattices. The analysis was conducted using a Bruker D8 Endeavor diffractometer.

Electromagnetic interference shielding efficiency

When electromagnetic waves come into contact with a shielding material like textiles, there are four potential outcomes: (1) absorption, where the electromagnetic waves are absorbed by the conductive or magnetic materials embedded in the textile, converting the energy into heat. (2) Reflection, where incoming electromagnetic waves bounce off the surface of the textile due to the difference in impedance between the textile and the surrounding medium. (3) Internal reflections refer to the sequence of multiple reflections occurring within the confines of the textile structure, serving to further diminish the intensity of the electromagnetic waves. (4) Transmission denotes the fraction of electromagnetic waves that are permitted to traverse the textile structure without being absorbed or reflected.

These processes together contribute to the material's total EMI SE. [Figure S4](#) depicts the interference model, illustrating the interaction between electromagnetic waves and the shielding medium. It demonstrates how these mechanisms contribute to reducing the penetration of electromagnetic waves through the shield. The above four processes, combined, contribute to the attenuation of the incident electromagnetic waves, and define the EMI SE of a material.

In this work, the EMI SE of the fabricated samples was measured using the rectangular waveguide method. Two rectangular waveguides (WR-90), two coaxial cables, and a vector network analyzer were used to sandwich the sample between the waveguides and quantify scattering parameters using the network analyzer. The dimensions of the hole in the waveguide were 10.2 mm in width and 22.9 mm in length. [Figure S5](#) displays the visual representation of the physical arrangement used to measure EMI SE. Measured scattering parameters were used to extract the sum of absorption (SE_A), reflection (SE_R), and multiple reflections (SE_M) contributions, which is applied to quantify overall shielding efficiency (SE_{total}). SE_{total} obtains from equation (1).³⁶

$$SE_{total}(dB) = SE_A + SE_R + SE_M \quad (1)$$

Due to the high conductivity, thin layer nature, and the X-band frequencies used, SE_M in the case of MXene coatings can be ignored, especially when $SE_A > 10$ dB or $SE_{total} > 15$ dB.^{37–39} The SE total is expressed as the following in equations (2) to (6):

$$SE_{total}(dB) = SE_A + SE_R \quad (2)$$

$$SE_A = -10 \log[\text{Tr}(1 - \text{Re})^{-1}] \quad (3)$$

$$SE_R = -10 \log(1 - \text{Re}) \quad (4)$$

$$\text{Tr} = |S_{21}|^2 = |S_{12}|^2 \quad (5)$$

$$\text{Re} = |S_{22}|^2 = |S_{11}|^2 \quad (6)$$

Where Tr and Re represent the transmission coefficient and reflection coefficient. S_{11} and S_{22} are the reflection coefficients at the input and output sides of the sample, respectively. These coefficients measure the amount of power reflected back at each side S_{21} and S_{12} represent the transmission coefficients, indicating the amount of power that passes through the sample from the input side to the output side and vice versa. In other words, S_{11} quantifies the reflected power at the input side, when the output side is ideally matched to the system impedance, while S_{22} quantifies the reflected power at the output side. S_{21} gives the transmission coefficient from the input to the output port, while S_{12} describes the transmission in the opposite direction. These coefficients are critical components of the S-parameter matrix, which is essential to characterizing the sample's EMI SE by evaluating how it absorbs, reflects, and transmits electromagnetic waves. Following the measurement of the EMI SE of untreated and 1-cycle coated fabrics, we decided to proceed with the second and third coating cycles for Full Milano and 1×1 Rib knit structures that exhibited the greatest EMI SE in each gauge category. Table 2 displays the specific information on the coating cycles for each fabric.

Results

Characteristics of hybrid knitted fabric treated with MXene

FESEM images reveal that the MXene coating has permeated the fabric, with noticeable deposition on both the embedded copper filament and the surrounding cotton fibers, indicating infiltration beyond the surface of the sample by the MXene coating.

EDS data of sample (T47) are presented in Figure 2(a) and show the elemental makeup of MXene as well as the copper (Cu) from the hybrid cotton sample. EDS elemental mapping provided in Figure S6 Shows the elemental mapping for uncoated sample and the sample coated with MXene and confirms a uniform distribution of the detected elements over the coated fabric surface compared to uncoated sample.

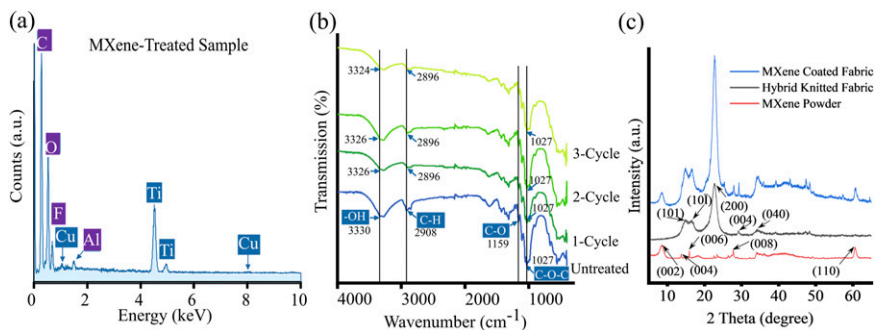


Figure 2. (a) EDS spectrum of the prepared sample (T47), (b) FTIR spectrum of a bare hybrid cotton sample (purple) (T17), and samples coated with 1 (red) (T35), 2 (orange) (T41), and 3 cycles (green) (T47) of MXene, respectively. (c) XRD pattern of MXene Powder (Ti_3C_2), uncoated hybrid fabric, and MXene coated hybrid fabric.

Figure 2(b) showcases FTIR spectroscopic analysis, detailing peaks that denote specific functional groups in the examined sample. At 1027 cm^{-1} , the peak suggests stretching vibrations typical of ether groups (C-O-C linkage). The peak at 1159 cm^{-1} signifies the C-O stretching vibration, commonly observed in alcohols, esters, or ethers. Additionally, a peak at 2908 cm^{-1} points to C-H stretching vibrations, and one at 3330 cm^{-1} aligns with the -OH stretching, frequently associated with alcohols and phenols. A slight shift in the hydroxyl group confirms that MXene sheets are attached to the surface of hybrid fabrics through hydrogen bonding. Although not detected by FTIR, it is also possible that additional bonding mechanisms are present between MXene and the cotton surface of the sample, in particular, van der Waals forces and electrostatic interactions, as reported earlier.^{40–42}

Figure 2(c) shows the XRD analysis of MXene powder, uncoated hybrid fabric, and MXene-coated hybrid fabric. For the MXene-coated hybrid fabric, the XRD pattern includes peaks from both the MXene and cotton components. Peaks at (004), (006), (008), and (110) correspond to the MXene coating, while peaks at (101), (10 $\bar{1}$), (200), (004), and (040) correspond to the cotton fabric. The presence of both sets of peaks in the coated fabric confirms the successful integration of MXene onto the cotton fibers.

Electromagnetic shielding efficiency performance of hybrid knitted fabrics

As can be seen from Figure 3 and the EDS mapping of the surface of the samples in Figure S6, the MXene sheets are uniformly distributed over the fibers of the sample. Uniform distribution of MXene sheets ensures their connectivity, which leads to better electrical characteristics and, in turn, better EMI SE performance. Moreover, as the gauge number increased, the samples exhibited a higher density, necessitating the use of additional copper filament and cotton for their fabrication. This increment in gauge not only amplifies the copper content within the samples but also correlates with a higher incorporation of MXene into the cotton matrix. The density and quality of the MXene coating,

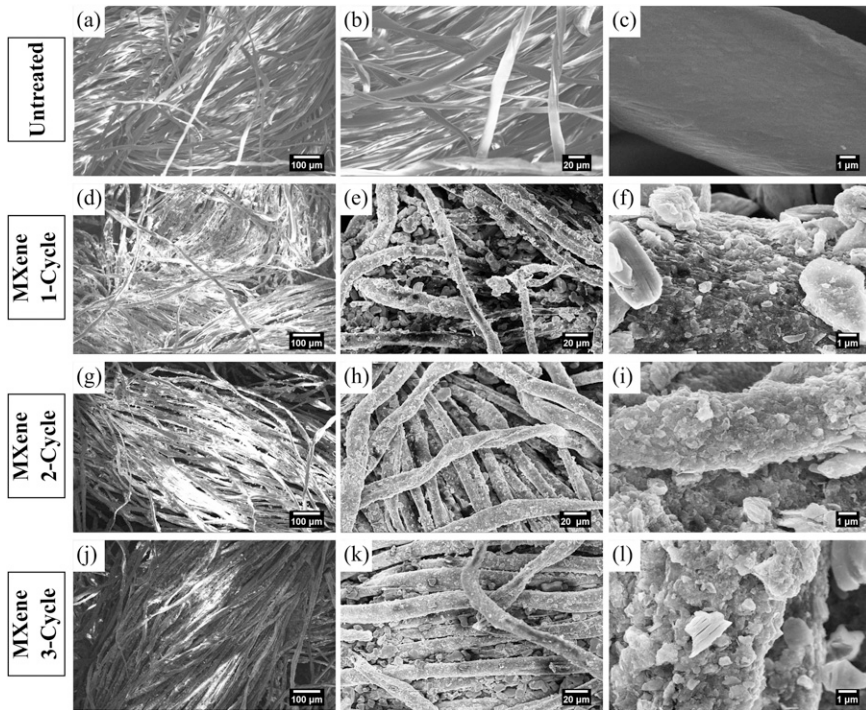


Figure 3. SEM images of fabric with a Full Milano knit pattern with a gauge of 12 and copper core diameter of 0.08 mm untreated and MXene-treated (T17, T35, T41, T47), (a-c) untreated (T17), (d-f) 1 coating cycle of MXene (T35), (g-i) 2 coating cycles of MXene (T41), (j-l) 3 coating cycles of MXene (T47).

alongside the increased copper content, synergistically lead to the superior EMI SE performance of these samples. Figure S7 to S9 in the Supplemental Material show the EMI SE of all samples with gauges 8, 10, and 12 in the frequency range of 8.2-12.4 GHz. EMI SE was quantified in the X-band frequency range (8.2-12.4 GHz). The measured scattering parameters acquired by the vector network analyzer were applied to equations (1) to (6) to calculate the overall EMI shielding efficiency. Five tests were conducted for each sample, and the mean value was reported as the EMI SE. In the frequency range of 8.2-12.4 GHz, the lowest EMI SE for each sample was recorded as the EMI SE sample. The mean value results and their standard deviation are displayed in Figures 4 and 5.

Effect of gauge on EMI SE. In the untreated samples, increasing the gauge from 8 to 12 enhanced the EMI SE, with Full Milano patterns showing an improvement from 12 dB to 16 dB, and 1×1 Rib structures exhibiting an increase from 10.5 dB to 14.9 dB, as indicated in Figures 4(a) and 5(a). For samples utilizing 0.07 mm copper core filaments (T3, T4, T9, T10, T15, and T16), a gauge range of 8 to 12 yielded EMI SE values ranging from 16.7 dB to 18.8 dB for Full Milano and 14.7 dB to 17.1 dB for 1×1 Rib structures,

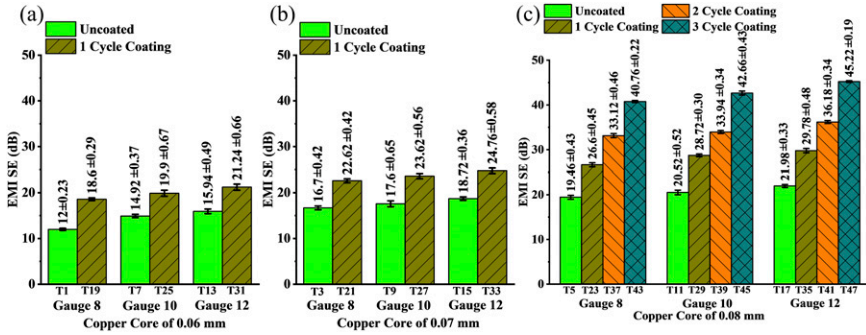


Figure 4. Effect of copper core diameter, gauge, and number of coating cycles on the EMI SE of a hybrid cotton textile with Full Milano knit pattern; (a) samples with 0.06 mm copper core diameter, (b) samples with 0.07 mm copper core diameter, (c) samples with 0.08 mm copper core diameter.

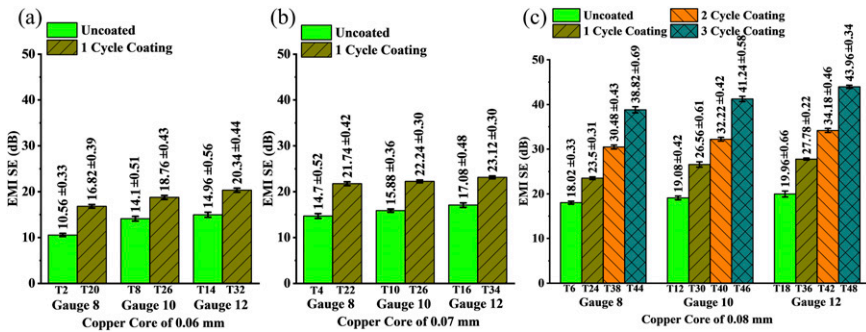


Figure 5. Effect of copper core diameter, gauge, and number of coating cycles on the EMI SE of a hybrid cotton textile with 1×1 Rib knit pattern; (a) samples with 0.06 mm copper core diameter, (b) samples with 0.07 mm copper core diameter, (c) samples with 0.08 mm copper core diameter.

respectively, as depicted in the same figures. Similarly, samples with 0.08 mm copper core filaments (T5, T6, T11, T12, T17, and T18) showed an increase in EMI SE from 16.7 dB to 18.8 dB for Full Milano and from 14.7 dB to 17.1 dB for 1×1 Rib structures, as detailed in Figures 4 and 5.

In the case of one-cycle MXene coating, textile samples fabricated with the 0.06 mm copper core filament (T19, T20, T25, T26, T31, and T32) exhibited EMI SE values of 18.5 dB to 21.3 dB and 16.8 dB to 20.3 dB for Full Milano and 1×1 Rib structure, respectively, with increasing gauge from 8 to 12, Figures 4 and 5. Similarly, samples with 0.07 mm copper core filament (T21, T22, T27, T28, T33, and T34) demonstrated EMI SE values of 22.5 dB to 24.8 dB for Full Milano, and 21.7 dB to 23.1 dB for 1×1 Rib structure, when the gauge increases from 8 to 12. Moreover, when a 0.08 mm copper core filament was used in the textile fabrication (T23, T24, T29, T30, T35, and T36),

increasing the gauge from 8 to 12 led to a rise in the EMI SE values from 26.5 dB to 29.7 dB for Full Milano, and 23.5 dB to 27.8 dB for the 1×1 Rib structure, as shown in Figures 4 and 5.

For samples with a 0.08 mm copper core filament (T37-T42) and subjected to a two-cycle MXene coating, an increase in the gauge from 8 to 12 enhanced the EMI SE from 33.1 dB to 36.2 dB for Full Milano structures and from 30.4 dB to 34.1 dB for 1×1 Rib structures, as demonstrated in Figures 4 and 5. Furthermore, with a three-cycle MXene coating, samples containing the 0.08 mm copper core filament (T43-T48) exhibited an elevation in EMI SE from 40.7 dB to 45.2 dB for Full Milano patterns and from 38.8 dB to 43.9 dB for 1×1 Rib patterns, upon increasing the gauge from 8 to 12, as shown in Figures 4 and 5.

In the uncoated copper-cotton hybrid knitted fabrics, the effect of increasing the gauge on EMI SE is an increase of about 2 dB. For the one cycle, 2 cycles, and 3 cycles coatings of MXene, the gauge effect became more significant with an increase in EMI SE reaching 3 dB, 4 dB, and 5 dB, respectively. Increasing the gauge number of a fabric leads to an increase in its density. This increment in density not only raises the quantity of copper present in the fabric but also extends the surface area present for coating. Furthermore, a higher gauge number correlates with reduced porosity of the textile, thereby enabling the application of more continuous and thicker MXene coatings. Such comprehensive coatings enhance the EMI SE of the fabric, as a denser and more continuous conductive layer offers greater resistance to electromagnetic penetration. Figure S7 to S9 show the EMI SE of fabrics based on their gauge number in the frequency range of 8.2-12.4 GHz (X-band frequency). Celen et al. utilized a circular knitting machine with gauges of 14 and 22 for EMI SE applications, observing a similar trend. Samples with the larger gauge demonstrated higher EMI SE values.⁴³ Huang et al. prepared knitted samples incorporating copper and stainless steel filaments using machine gauges of 3.5 and 7. Their findings indicated that samples produced with the higher gauge exhibited better EMI SE values.⁴⁴ This observation aligns with the established understanding that higher gauges, which create denser fabric structures, tend to enhance the EMI SE due to the increased presence of conductive material in the fabric matrix.

Effect of knit pattern on EMI SE. Figures 4 and 5 exhibit the influence of the knit pattern on EMI SE, with Figure 4 showing the EMI SE for the Full Milano knit pattern and Figure 5 showing the EMI SE for the 1×1 Rib knit pattern. The results indicate that the EMI SE of the Full Milano knit structure is roughly 2 to 3 dB higher than that of the 1×1 Rib knit counterpart samples. The significant differences observed can be primarily attributed to the denser construction of the Full Milano knit samples, which feature two extra courses of tuck knit stitches compared to the 1×1 Rib knit pattern. This structure provides an increased surface area comprised of cotton fibers, consumes more copper filaments, as well as added depth. These factors together facilitate the application of a more substantial and continuous layer of MXene coating compared to the 1×1 Rib knit pattern. Consequently, the Full Milano samples exhibit a more pronounced thickness in MXene deposition, enhancing the overall electromagnetic shielding performance. Figure 6

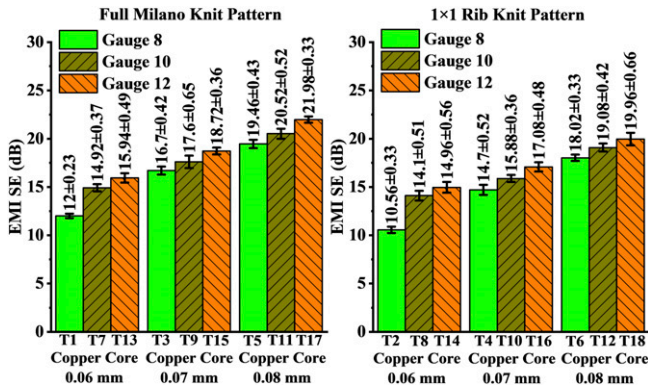


Figure 6. Effect of knit pattern on the EMI SE of samples with the Full Milano and 1 × 1 Rib knit pattern.

Table 3. Categorized efficiency of electromagnetic shielding of textiles.

Electromagnetic Efficiency	Excellent (dB)	Very good (dB)	Good (dB)	Moderate (dB)	Fair (dB)
Professional use	SE > 60 dB	60 dB ≥ SE > 50 dB	50 dB ≥ SE > 40 dB	40 dB ≥ SE > 30 dB	30 dB ≥ SE > 20 dB
General use	SE > 30 dB	30 dB ≥ SE > 20 dB	20 dB ≥ SE > 10 dB	10 dB ≥ SE > 7 dB	10 dB ≥ SE > 7 dB

illustrates the effect of different knit patterns on the EMI SE of the uncoated hybrid fabrics.

Effect of copper core diameter on EMI SE. The effect of copper core on EMI SE in the uncoated samples is shown in Figures 4 and 5. The increase in the copper core diameter from 0.06 mm to 0.08 mm enhances the EMI SE of the samples by 5 to 8 dB. The correlation between the diameter of copper filaments integrated into cotton samples and the improvement in EMI SE can be explained by several crucial parameters. Increasing the diameter of copper filaments results in an enhanced electrical conductivity of the fabric, which improves the reflection of incident electromagnetic waves, which is crucial for effective EMI shielding. Furthermore, the increased diameter offers a greater surface area for the deposition of MXene, facilitating the formation of a more uniform and continuous (less porous) conductive layer, which is essential for efficient shielding. Additionally, the presence of thicker copper filaments allows a facile movement of induced currents, which play a crucial role in redirecting incident electromagnetic energy away from the textile surface. Lai et al. used Stainless Steel filament with diameter of 0.08 mm in the structure of hybrid yarn and obtained EMI SE of 5 to 20 dB in the frequency range of 0-3 GHz. In our research work we obtained a higher EMI SE of more than 45 dB in a higher frequency range.³² Another study reported that knitted samples produced with a machine gauge of 7 using hybrid copper/PET yarns, featuring a copper diameter of 0.08 mm, achieved a maximum EMI SE of 14 dB with a 2-layer lamination,

17 dB with a 3-layer lamination, and 17 dB with a 4-layer lamination.⁴⁴ In comparison, our samples demonstrate significantly higher EMI SE values due to the use of a knitting machine with a higher gauge of 8, 10, and 12 needle per inch. The higher gauge creates a denser and more tightly knit fabric, which enhances the overall EMI SE. This improved performance is attributed to the increased density of conductive pathways provided by the higher gauge knitting, which offers better attenuation of electromagnetic waves.

Effect of coating cycles on EMI SE. The number of coating cycles influences EMI SE. In fact, this aspect was the most prominent contributor to the efficiency of the sample to attenuate frequencies in the X-band. For example, the EMI SE of the samples after 3 coating cycles is twice higher than that of the untreated samples, as shown in [Figures 4 and 5](#).

After one-cycle MXene coating on the Full Milano knit pattern with a core diameter of 0.06 mm (T19, T25, T31), EMI SE increased by an average of 40.6% compared to uncoated counterparts (T1, T7, T13). For the Full Milano knit pattern incorporating a 0.07 mm core diameter (Samples T21, T27, T33), there was an increase in EMI SE of 35.2% relative to the uncoated baseline samples (T3, T9, T15). Moreover, the Full Milano knit pattern with a core diameter of 0.08 mm (T23, T29, T35) demonstrated an EMI SE increase by an average of 36.9% compared to their corresponding plain hybrid cotton samples (T5, T11, T17). For the 1×1 Rib knit pattern featuring a 0.06 mm copper core diameter (Samples T20, T26, T32), a single coating cycle of MXene resulted in an average EMI SE increase of 42.6% over the uncoated control samples (T2, T8, T14). Similarly, for the 1×1 Rib knit pattern with a 0.07 mm copper core diameter (T22, T28, T34), there was an average EMI SE increase of 40.7% when compared to their respective uncoated controls (T4, T10, T16). Lastly, for a 0.08 mm copper core diameter in the 1×1 Rib knit pattern (T24, T30, T36), the EMI SE was enhanced by an average of 36.5% relative to the uncoated samples (T6, T12, T18).

Further increase in EMI SE with increasing MXene coating cycles is observed for both knit patterns. For example, upon completing two coating cycles on the Full Milano knit pattern with a 0.08 mm copper core diameter (T37, T39, T41), the EMI SE experienced an average increase of 66.5% over the uncoated base samples (T5, T11, T17). A similar enhancement was observed for the 1×1 Rib knit pattern with a 0.08 mm copper core diameter (T38, T40, T42), where the EMI SE increased by an average of 69.6% compared to their uncoated counterparts (T6, T12, T18). A more pronounced improvement occurred after three coating cycles on the Full Milano knit pattern with a 0.08 mm core diameter (T43, T45, T47), resulting in an average EMI SE increase of 107.5% relative to the uncoated textiles (T5, T11, T17). Additionally, the 1×1 Rib knit pattern with a 0.08 mm copper core diameter (T44, T46, T48) underwent a remarkable average increase of 117.6% in EMI SE after three coating cycles when compared to the uncoated samples (T6, T12, T18), underlining the efficacy of multiple MXene coatings in enhancing EMI shielding in textiles.

Discussion

Our results indicate that the EMI SE of hybrid copper-cotton textiles is influenced by several factors, including the textile gauge, copper core diameter, knit pattern, and MXene coating cycles. However, the experimental findings reveal a significant correlation between the number of MXene coating cycles and the measured EMI SE of the textile samples, particularly within the X-band frequency range. The substantial enhancement in EMI SE observed after three coating cycles, resulting in more than a twofold increase compared to untreated samples, strongly demonstrates the crucial role of coating cycles.

Augmentation of copper core diameters within textile structures yields a multiplicity of advantages for the amplification of electromagnetic interference shielding effectiveness (EMI SE). Initially, this adjustment enhances the material's electrical conductivity through the integration of a greater quantity of conductive material, thereby facilitating the efficient reflection and absorption of electromagnetic waves. In addition, the increase in surface area enhances the degree of interaction between the electromagnetic waves and the conductive material, thereby reinforcing the fabric's shielding efficacy. Conclusively, improved inter-fiber contact enhances the conductivity pathways within the fabric, culminating in a comprehensive enhancement of EMI shielding performance.

Enhancement of the MXene coating cycles on fabric substrates provides a strategic avenue to bolster EMI SE via a spectrum of mechanisms. Primarily, this increase in coating cycles broadens the coverage (and thickness of the coating), ensuring that a more extensive region of the fabric is fortified. Subsequently, it intensifies the absorption and reflection capabilities of electromagnetic waves, a consequence of the presence of denser MXene layers. Furthermore, this process boosts the conductivity, thereby enabling a more efficient dissipation of electromagnetic energy. Ultimately, it affords the precision tuning of the MXene layer thickness, a critical factor in optimizing shielding effectiveness.

By increasing the knitting machine gauge, the resulting textiles become thicker and denser. This allows for a greater amount of copper wire to be incorporated into the fabric's structure, as well as providing a larger amount of cotton for the deposition of MXene. This will lead to an augmentation in the EMI SE of the fabric.

In the case of the Full Milano knit pattern, which has several core diameters (0.06 mm, 0.07 mm, and 0.08 mm), each additional coating cycle resulted in a significant increase in EMI SE. The largest copper core diameter of 0.08 mm demonstrated the greatest improvement in EMI SE after three coatings cycles of MXene.

These results can be explained by the increase in MXene interconnected networks that grow more prominent with each subsequent layer, resulting in enhanced surface coverage and improved capacity to reflect and absorb electromagnetic radiation. The more compact structure of the Full Milano knit pattern, along with the larger copper core filaments that offer a greater surface area, leads to a less porous substrate base for MXene application. This ultimately leads to enhanced MXene coatings and, in turn, EMI shielding. Moreover, the Full Milano pattern dual-layered knit provides greater depth for MXene penetration, potentially accounting for the variations in EMI shielding enhancements observed between the Full Milano and the 1×1 Rib knit patterns. The 1×1 Rib structure may have a lower fabric depth compared to Full Milano, potentially resulting in a lower increase of

EMI SE. Nevertheless, both structures exhibit significant enhancements when additional MXene coatings are applied, suggesting that the efficiency of MXene as a shielding material depends not only on the quantity used but also on the structural properties of the textile substrate.

In order to examine the impact of factors such as copper diameter, gauge, and number of coating on EMI SE, we used mean values along with 95% confidence intervals. Additionally, we calculated the mean value, standard deviation, and standard error of the tested samples. The findings of the 95% confidence intervals in Table S2 and S3 indicate a statistically significant difference in EMI SE as a consequence of the variable being evaluated.

The Committee for Conformity Assessment on Accreditation and Certification of Functional and Technical Textiles has defined specified requirements for the electromagnetic shielding of textiles (Table 3). Two categories of general and professional use are defined for the EMI SE of fabrics. The general use such as casual wear, office uniforms, maternity dresses, aprons, consumptive electronic products, and communication-related products. The *professional use* includes medical equipment, quarantine material, the professional security uniform for the electronic manufacturer, and the electronic kit. Based on Table 3, all the uncoated samples are assessed as 'Good' for *general use*, all the 1-cycle coated samples are in the 'Very Good' category for general use, all the 2-cycle coated samples are characterized as 'Excellent' for general use, and 3-cycle coated samples are categorized as 'Good' for the professional use.^{45,46} By judicious choice of textile substrates and controlling the number of MXene coating cycles, it is feasible to customize the properties of MXene-coated fabrics to fulfill the need of commercial applications with specific EMI SE criteria. By using highly conductive, single-flake MXene, such as carbonitride Ti_3CNT_x MXene, considerable improvements in the EMI SE of these textiles can be realized.⁴⁷

Conclusions

This research presented a comprehensive study involving designing hybrid knitted fabrics utilizing copper-cotton core-spun yarns coated with MXene. The design approach took into account four specific factors to determine their impact on the EMI SE of the samples produced. The variables encompassed in this study are the copper core diameter, the textile knit pattern, the knitting machine gauge, and the number of MXene coating cycles applied to the textiles. Compared to prior studies, incorporating copper filaments and MXene sheets resulted in high EMI SE with fewer coating cycles. The study concluded that the number of coating cycles has the most significant influence on the EMI SE of given samples. Samples with three coating cycles of MXene have an EMI SE that is more than twice as large as uncoated samples. The EMI SE of prepared textiles with the Full Milano knit pattern is greater than that of prepared fabrics with the 1×1 Rib knit pattern. The difference between these two knit patterns is approximately 2 to 3 dB. Moreover, increasing the copper core thickness and gauge of fabric resulted in an increase in the maximum EMI SE of developed textiles. The knit pattern has some impact but is not as pronounced as the other three factors mentioned above. Future research should focus on

the long-term stability of MXene coatings under various environmental conditions, the scalability of the coating process, and integration into large-scale textile manufacturing. Additionally, practical applications in aerospace, telecommunications, and wearable electronics, supported by field testing, could validate the effectiveness of these high-performance EMI shielding fabrics in real-world scenarios.

Declaration of conflicting interests

The author(s) declared no potential conflicts of interest with respect to the research, authorship, and/or publication of this article.

Funding

The author(s) disclosed receipt of the following financial support for the research, authorship, and/or publication of this article: This research was funded Canadian government through the Canada Foundation for Innovation (JELF) Grant, Canada Research Chair (Tier 1) (award # 950-231466), and NSERC Discovery Grant (award # RGPIN-2020-06970).

ORCID iD

Hamed Mohammadi Mofarah  <https://orcid.org/0000-0001-5942-2329>

Supplemental material

Supplemental material for this article is available online.

References

1. Shekhirev M, Shuck CE, Sarycheva A, et al. Characterization of MXenes at every step, from their precursors to single flakes and assembled films. *Prog Mater Sci* 2021; 120: 100757.
2. Yin L, Yang Y, Yang H, et al. Rapid foaming of dense MXene films induced by acid-base neutralization reaction. *Cell Reports Physical Science* 2023; 4: 101421.
3. Luo J, Gao S, Luo H, et al. Superhydrophobic and breathable smart MXene-based textile for multifunctional wearable sensing electronics. *Chem Eng J* 2021; 406: 126898.
4. Wang Q-W, Zhang H-B, Liu J, et al. Multifunctional and water-resistant MXene-decorated polyester textiles with outstanding electromagnetic interference shielding and joule heating performances. *Adv Funct Mater* 2019; 29: 1806819.
5. Liu L, Chen W, Zhang H, et al. Flexible and multifunctional silk textiles with biomimetic leaf-like MXene/silver nanowire nanostructures for electromagnetic interference shielding, humidity monitoring, and self-derived hydrophobicity. *Adv Funct Mater* 2019; 29: 1905197.
6. Zheng X, Zhou X, Xu J, et al. Highly stretchable CNT/MnO₂ nanosheets fiber supercapacitors with high energy density. *J Mater Sci* 2020; 55: 8251–8263.
7. Polat EO, Mercier G, Nikitskiy I, et al. Flexible graphene photodetectors for wearable fitness monitoring. *Sci Adv* 2019; 5: eaaw7846.
8. Xu C, Zhang X, Liu S, et al. Selected phase separation renders high strength and toughness to polyacrylamide/alginate hydrogels with large-scale cross-linking zones. *ACS Appl Mater Interfaces* 2021; 13: 25383–25391.

9. Abulikemu M, Tabrizi BEA, Ghobadloo SM, et al. Silver nanoparticle-decorated personal protective equipment for inhibiting human coronavirus infectivity. *ACS Appl Nano Mater* 2022; 5: 309–317.
10. He Y, Zhou M, Mahmoud MHH, et al. Multifunctional wearable strain/pressure sensor based on conductive carbon nanotubes/silk nonwoven fabric with high durability and low detection limit. *Adv Compos Hybrid Mater* 2022; 5: 1939–1950.
11. Ge F, Fei L, Zhang J, et al. The electrical-triggered high contrast and reversible color-changing janus fabric based on double side coating. *ACS Appl Mater Interfaces* 2020; 12: 21854–21862.
12. Ren J, Wang C, Zhang X, et al. Environmentally-friendly conductive cotton fabric as flexible strain sensor based on hot press reduced graphene oxide. *Carbon* 2017; 111: 622–630.
13. Wang H, Niu H, Zhou H, et al. Multifunctional directional water transport fabrics with moisture sensing capability. *ACS Appl Mater Interfaces* 2019; 11: 22878–22884.
14. Lima RMAP, Alcaraz-Espinoza JJ, da Silva FAG, et al. Multifunctional wearable electronic textiles using cotton fibers with polypyrrole and carbon nanotubes. *ACS Appl Mater Interfaces* 2018; 10: 13783–13795.
15. Ghosh S, Nitin B, Remanan S, et al. A multifunctional smart textile derived from merino wool/nylon polymer nanocomposites as next generation microwave absorber and soft touch sensor. *ACS Appl Mater Interfaces* 2020; 12: 17988–18001.
16. Zhang X, Wang X, Lei Z, et al. Flexible MXene-decorated fabric with interwoven conductive networks for integrated joule heating, electromagnetic interference shielding, and strain sensing performances. *ACS Appl Mater Interfaces* 2020; 12: 14459–14467.
17. Uzun S, Han M, Strobel CJ, et al. Highly conductive and scalable Ti3C2T-coated fabrics for efficient electromagnetic interference shielding. *Carbon* 2021; 174: 382–389.
18. Ghidui M, Lukatskaya MR, Zhao M-Q, et al. Conductive two-dimensional titanium carbide ‘clay’ with high volumetric capacitance. *Nature* 2014; 516: 78–81.
19. Shahzad F, Alhabeab M, Hatter CB, et al. Electromagnetic interference shielding with 2D transition metal carbides (MXenes). *Science* 2016; 353: 1137–1140.
20. Zhang Y-Z, Lee KH, Anjum DH, et al. MXenes stretch hydrogel sensor performance to new limits. *Sci Adv* 2018; 4: eaat0098.
21. Jiang Y, Xie X, Chen Y, et al. Hierarchically structured cellulose aerogels with interconnected MXene networks and their enhanced microwave absorption properties. *J Mater Chem C* 2018; 6: 8679–8687.
22. Liu J, Zhang H-B, Sun R, et al. Hydrophobic, flexible, and lightweight MXene foams for high-performance electromagnetic-interference shielding. *Adv Mater* 2017; 29: 1702367.
23. Guo Y, Zhong M, Fang Z, et al. A wearable transient pressure sensor made with MXene nanosheets for sensitive broad-range human-machine interfacing. *Nano Lett* 2019; 19: 1143–1150.
24. Yin G, Wang Y, Wang W, et al. A flexible electromagnetic interference shielding fabric prepared by construction of PANI/MXene conductive network via layer-by-layer assembly. *Adv Mater Interfac* 2021; 8: 2001893.
25. Li D-Y, Liu L-X, Wang Q-W, et al. Functional polyaniline/MXene/cotton fabrics with acid/alkali-responsive and tunable electromagnetic interference shielding performances. *ACS Appl Mater Interfaces* 2022; 14: 12703–12712.

26. Dong J, Luo S, Ning S, et al. MXene-coated wrinkled fabrics for stretchable and multi-functional electromagnetic interference shielding and electro/photo-thermal conversion applications. *ACS Appl Mater Interfaces* 2021; 13: 60478–60488.
27. Lan C, Jia H, Qiu M, et al. Ultrathin MXene/polymer coatings with an alternating structure on fabrics for enhanced electromagnetic interference shielding and fire-resistant protective performances. *ACS Appl Mater Interfaces* 2021; 13: 38761–38772.
28. Choi HK, Lee A, Park M, et al. Hierarchical porous film with layer-by-layer assembly of 2D copper nanosheets for ultimate electromagnetic interference shielding. *ACS Nano* 2021; 15: 829–839.
29. Verma R, Thakur P, Chauhan A, et al. A review on MXene and its' composites for electromagnetic interference (EMI) shielding applications. *Carbon* 2023; 208: 170–190.
30. Tunakova V, Tunak M, Bajzik V, et al. Hybrid knitted fabric for electromagnetic radiation shielding. *Journal of Engineered Fibers and Fabrics* 2020; 15: 155892502092539.
31. Jagatheesan K, Ramasamy A, Das A, et al. Electromagnetic shielding effectiveness of carbon/stainless steel/polypropylene hybrid yarn-based knitted fabrics and their composites. *J Text Inst* 2018; 109: 1445–1457.
32. Lai M-F, Lou C-W, Lin TA, et al. High-strength conductive yarns and fabrics: mechanical properties, electromagnetic interference shielding effectiveness, and manufacturing techniques. *J Text Inst* 2021; 112: 347–357.
33. Mofarah HM, Najar SS and Etrati SM. Mechanical properties of copper/cotton core-spun yarns produced by siro and ring spinning methods. *Indian J Fibre Text Res* 2019; 44: 431–436.
34. Mohammadi Mofarah H, Shaikhzadeh Najar S and Etrati SM. Investigating the electromagnetic shielding effectiveness of copper/cotton full Milano and 1×1 rib weft-knitted fabrics. *J Text Inst* 2019; 110: 891–900.
35. Ghosh S, Reman S, Mondal S, et al. An approach to prepare mechanically robust full IPN strengthened conductive cotton fabric for high strain tolerant electromagnetic interference shielding. *Chem Eng J* 2018; 344: 138–154.
36. Ahmad AF, Abbas Z, Obaiys SJ, et al. Effect of untreated fiber loading on the thermal, mechanical, dielectric, and microwave absorption properties of polycaprolactone reinforced with oil palm empty fruit bunch biocomposites. *Polym Compos* 2018; 39: E1778–E1787.
37. Yin G, Wang Y, Wang W, et al. A flexible electromagnetic interference shielding fabric prepared by construction of PANI/MXene conductive network via layer-by-layer assembly. *Adv Mater Interfac* 2021; 8: 2001893.
38. Saini P, Choudhary V, Singh BP, et al. Polyaniline–MWCNT nanocomposites for microwave absorption and EMI shielding. *Mater Chem Phys* 2009; 113: 919–926.
39. Pande S, Singh B, Mathur R, et al. Improved electromagnetic interference shielding properties of MWCNT–PMMA composites using layered structures. *Nanoscale Res Lett* 2009; 4: 327–334.
40. Repon MR, Islam T, Sadia HT, et al. Development of antimicrobial cotton fabric impregnating AgNPs utilizing contemporary practice. *Coatings* 2021; 11: 1413.
41. Tania IS, Ali M and Azam MS. In-situ synthesis and characterization of silver nanoparticle decorated cotton knitted fabric for antibacterial activity and improved dyeing performance. *SN Appl Sci* 2019; 1: 64.

42. Hasan KMF, Horváth PG, Kóczán Z, et al. Colorful and facile in situ nanosilver coating on sisal/cotton interwoven fabrics mediated from European larch heartwood. *Sci Rep* 2021; 11: 22397.
43. Celen R and Ulcay Y. Investigating electromagnetic shielding effectiveness of knitted fabrics made by barium titanate/polyester bicomponent yarn. *Journal of Engineered Fibers and Fabrics* 2019; 14: 155892501983780.
44. Huang C-H, Lin J-H, Yang R-B, et al. Metal/PET composite knitted fabrics and composites: structural design and electromagnetic shielding effectiveness. *J Electron Mater* 2012; 41: 2267–2273.
45. Committee for Conformity Assessment on Accreditation and Certification of Functional and Technical Textiles. *Specified requirements of electromagnetic shielding textiles*, 2003. <https://www.ftts.org.tw/images/fa003E.pdf>
46. Šafářová V, Tunák M, Truhlář M, et al. A new method and apparatus for evaluating the electromagnetic shielding effectiveness of textiles. *Textil Res J* 2016; 86: 44–56.
47. Iqbal A, Shahzad F, Hantanasirisakul K, et al. Anomalous absorption of electromagnetic waves by 2D transition metal carbonitride Ti₃CNT_x (MXene). *Science* 2020; 369(6502): 446–450.